

Experimental Study on the Heat Transfer Performance of Al_2O_3 - Ethylene Glycol/Water-Based Nanofluid as Coolant in Vehicle Radiator

Surya Prasad Adhikaria*, Aanchal Gupta^a, Puskar Chhetria, Saksham Subedia

^aDepartment of Mechanical and Aerospace Engineering, Pulchowk Campus, Institute of Engineering, Tribhuvan University, Kathmandu, 44700, Nepal

*Corresponding Author (spadhikari@pcampus.edu.np)

Abstract- In this research, the heat transfer efficiency of the vehicle radiator cooling system was experimentally investigated by mixing at different volume concentrations of an aluminum oxide (Al_2O_3) nanoparticle (NPs) in the regular coolant i.e. a 1:2 ratio mixture of ethylene glycol and distilled water. The sol-gel process was used to synthesize the NPs and characterized using UV-Vis spectroscopy. TATA TIAGO XZ+ was used for this investigation in an idling condition and remained motionless throughout the test. Inlet air temperature, flow rate, outlet temperature, and surface temperature were all recorded at different concentrations of NPs. Experimental results showed that the overall heat transfer coefficient of the nanofluids was improved by 33.63%, 65.4%, and 83.5% at 0.2%, 0.5%, and 1% concentrations, respectively. Thus, the results displayed that the cooling capacity can be increased with the increment of Al_2O_3 NPs concentration within a certain range in the normal coolant.

Keywords: Radiator, Coolant, Nanomaterials, Nanofluid, Heat transfer coefficient

© Copyright 2025 Authors - This is an Open Access article published under the Creative Commons Attribution License (<http://creativecommons.org/licenses/by/3.0>). Unrestricted use, distribution, and reproduction in any medium are permitted, provided the original work is properly cited.

1. Introduction

The engine cooling system plays a critical role in absorbing the excess heat generated within the internal combustion (IC) engine. It does so by circulating a coolant fluid through cooling passages

around the engine block, thereby maintaining an optimal operating temperature and preventing potential engine damage. During the combustion process, fuel releases a substantial amount of heat within the combustion chamber. However, to ensure safe operation and optimal engine performance, it is essential to regulate this temperature. If excess heat is not effectively dissipated, the engine temperature can rise to uncontrollable levels, potentially leading to damage to engine components or complete engine failure [1]. Generally, the coolant flows through tubes or water jackets surrounding the engine to absorb excess heat, which is then released into the external environment; a region of lower temperature [2]. If this excess heat is not effectively dissipated, it can increase stress on engine components by lowering the viscosity of the lubricating oil, potentially resulting in significant engine malfunctions or even failure [3]. The main components of the engine cooling system include the radiator, water pump, cooling fan, pressure cap, and thermostat valve. Each of these parts plays a vital role in regulating engine temperature by ensuring efficient circulation, heat exchange, and pressure control within the system [4]. The cooling effect in an engine is generally achieved by circulating coolant through dedicated cooling passages around the engine block. As the coolant flows through various engine components, it absorbs the excess heat generated during operation. This heated coolant then returns to the radiator, where it releases the absorbed heat to the surrounding air. Once cooled, the low-temperature coolant is recirculated back into the engine. This continuous

cycle helps maintain the engine at an optimal operating temperature, ensuring both efficiency and protection against overheating [5]. In water-cooled engines, a proper mixture of ethylene glycol or propylene glycol with water is commonly used as a coolant. These organic compounds, when blended with water in suitable proportions, exhibit high specific heat capacities. This property enables them to absorb and transfer significant amounts of heat, making them ideal for maintaining stable engine temperatures. Their excellent thermal properties are the primary reason for their widespread use in engine cooling systems [6].

NPs are solid particles with sizes typically ranging from 1 to 100 nanometers (nm). Due to their extremely small size and high surface area, they exhibit excellent dispersion properties, allowing them to mix uniformly and remain stable in conventional coolants without settling or agglomerating [7]. The addition of NPs to conventional coolants has been found to significantly influence the Reynolds number, leading to enhanced heat transfer efficiency. This improvement is primarily attributed to the altered thermophysical properties of the nanofluid, such as increased thermal conductivity and modified viscosity. As a result, numerous researchers have explored the incorporation of various metal oxide NPs into standard coolants to achieve higher heat transfer coefficients and optimize the performance of thermal systems [8], [9], [10].

Among the various techniques available for synthesizing metal oxide NPs, such as vapor phase compression, mechanical alloying, plasma methods, and electrochemical processes, the sol-gel method stands out as the most widely adopted. This popularity is largely due to its distinct advantages, including the ability to simultaneously produce multiple types of NPs, excellent control over particle size and morphology, and the formation of highly homogeneous composites with superior purity. Additionally, the sol-gel process operates at relatively low processing temperatures, making it energy-efficient, and it is scalable for industrial production, further enhancing its suitability for both research and commercial applications [11], [12], [13], [14], [15]. Ghosh et al. synthesized CuAlO_2 nanocrystalline powders using two different methods and conducted a comparative analysis of the resulting particle sizes. Their findings revealed that the NPs produced via the nitrate-citrate sol-gel technique were significantly

smaller in size compared to those synthesized using the solid-state reaction method, highlighting the effectiveness of the sol-gel process in achieving finer particle dimensions [16]. Similarly, S. Tabesh et al. successfully synthesized $\gamma\text{-Al}_2\text{O}_3$ NPs using an improved sol-gel method. In this approach, they employed a novel combination of precursors including aluminum nitrate, ethylene glycol, citric acid (CA), and triethanolamine (TEA), which contributed to better control over the synthesis process. The resulting $\gamma\text{-Al}_2\text{O}_3$ nanoparticles exhibited particle sizes in the range of approximately 6 to 13 nanometers, indicating the effectiveness of the modified sol-gel technique in producing ultra-fine and uniform nanostructures [17].

A majority of previous studies have indicated that among various types of metal oxide NPs, Al_2O_3 NPs are particularly effective in enhancing the heat transfer properties of conventional coolants. This superior performance is attributed to their favorable thermal conductivity, stability, and dispersion characteristics. For instance, D. Chavan et al. demonstrated that incorporating Al_2O_3 NPs at a 1% volume concentration into a base coolant led to a significant enhancement in thermal performance. Under controlled conditions, where both the Reynolds number and mass flow rate were kept constant, the heat transfer rate increased by approximately 40%, while the overall heat transfer coefficient saw an improvement of around 36%. These findings highlight the potential of Al_2O_3 -based nanofluids for more efficient thermal management in various engineering applications [18]. Elias et al. investigated the effect of incorporating Al_2O_3 NPs into a base fluid composed of water and ethylene glycol, varying the NPs volume concentration from 0 to 1 vol.%. They conducted a series of experimental measurements to evaluate the thermal conductivity, viscosity, density, and specific heat capacity of the resulting nanofluids across different temperature ranges. The results revealed that thermal conductivity, density, and viscosity all increased proportionally with higher NPs concentrations, indicating improved heat transfer potential. However, a notable decrease in specific heat capacity was observed at higher concentrations of Al_2O_3 , likely due to the reduced heat-storing ability of the fluid as more solid particles were added [19]. Similarly, K. P. Vasudevan Nambesan et al. explored the thermal performance of nanofluids prepared with 90:10 and 80:20 water-to-ethylene glycol ratios,

incorporating 0.1% Al_2O_3 NPs. Their findings demonstrated a remarkable 37% improvement in heat transfer performance, underscoring the synergistic effects of NPs addition and base fluid composition [20]. Furthermore, additional studies have shown that the enhancement in the thermal properties of nanofluids is influenced not only by the NPs volume concentration but also by the particle size. Smaller NPs, due to their larger surface area-to-volume ratio, tend to interact more effectively with the base fluid, thereby contributing more significantly to the overall thermal conductivity improvement [21].

S. Mukherjee et al. conducted an experimental study by dispersing SiO_2 NPs into engine coolant at varying mass concentrations. Their results demonstrated that both the heat transfer performance and thermal efficiency improved with increasing NPs concentration and flow temperature, highlighting the combined impact of thermal conditions and NPs loading on system performance [22]. Similarly, Eastman et al. reported a substantial enhancement in thermal performance by incorporating just 0.3% volume concentration of copper (Cu) NPs into ethylene glycol. The addition of these highly conductive NPs led to an impressive 45% increase in thermal conductivity, emphasizing the potential of metallic NPs in nanofluid development [23].

Hashemabadi et al. further explored the impact of Al_2O_3 NPs dispersed separately in ethylene glycol and water. Their findings revealed a 40% increase in both heat transfer performance and Reynolds number upon NPs addition. More importantly, their study concluded that the enhancement in thermal performance was more strongly influenced by the volume concentration of NPs than by temperature variations, underlining the dominant role of NPs loading in improving heat transfer [24]. Ali et al. investigated the cooling performance of MgO -based nanofluids at various volume concentrations ranging from 0.06% to 0.12%, while maintaining flow rates between 8 and 16 liters per minute. The study reported a maximum increase of 31% in thermal performance at NPs concentrations of 0.12%, indicating the strong potential of MgO NPs for cooling applications [25].

Wen et al. focused on the convective heat transfer behavior of Al_2O_3 nanofluids under laminar flow conditions. Using a tube with an internal diameter of 4.5 mm, they tested nanofluids at 0.6%,

1%, and 1.6% volume concentrations. The results showed a significant improvement in heat transfer efficiency with increasing NPs concentration, confirming the effectiveness of Al_2O_3 nanofluids in enhancing convective heat transfer under controlled flow conditions [26].

The aforementioned studies collectively highlight that the application of NPs extends far beyond a single domain, evolving into a rapidly growing interdisciplinary field that bridges science and engineering. Among these advancements, enhancing the thermal performance of conventional coolants through the strategic addition of NPs, particularly at optimized concentrations, has emerged as a promising approach. This strategy holds significant potential for improving the efficiency of internal combustion (IC) engine cooling systems, a critical area in automotive thermal management.

Numerous previous investigations have demonstrated that incorporating Al_2O_3 NPs into standard coolants leads to improved heat transfer characteristics. These studies have employed varying concentrations of Al_2O_3 NPs and reported different degrees of enhancement in thermal performance, depending on the NPs loading and experimental conditions. However, despite the growing body of research, there remains a notable gap: no experimental study has yet evaluated the thermal performance of Al_2O_3 -based nanofluids as coolants in a live, functioning engine environment.

The objective of this experimental research is to address this gap by assessing the heat transfer performance of nanofluids formulated by dispersing Al_2O_3 NPs at different volume concentrations into a conventional coolant. In this study, Al_2O_3 NPs were synthesized using the sol-gel method and subsequently mixed with a base coolant consisting of 33.33% ethylene glycol and 66.67% distilled water. The resulting nanofluids, prepared at varying concentrations, were tested in a real-world automotive setup using a TATA TIAGO XZ+ vehicle under idling conditions. The focus was to evaluate how the NP-enhanced coolant performs in terms of heat transfer efficiency within an actual engine cooling system.

2. Experimental and Mathematical Modelling Procedures

2.1 Vehicle Specification and Setup

The **TIAGO XZ+ 2016 model** was used as the experimental vehicle for this study. It is

equipped with a 1199 cc petrol engine featuring a 4-cylinder Dual Overhead Camshaft (DOHC) configuration. The engine delivers a maximum power output of **84 BHP at 6000 rpm** and a peak torque of **114 Nm at 3500 rpm**.



Figure1: TIAGO XZ+ 2016 model

2.2 Preparation of NPs

Al_2O_3 NPs were synthesized using the sol-gel method. To prepare a 0.1 M ethanolic solution of aluminum trichloride (AlCl_3), 13.34g of AlCl_3 was dissolved in ethanol and stirred using a magnetic stirrer for 30 minutes. Subsequently, 50 mL of distilled water was added to the solution to initiate sol formation. To facilitate gelation and promote the formation of interconnected NPs, a 25% ammonia (NH_3) solution was gradually added during continued stirring. The resulting gel was then left at room temperature for 30 hours to allow aging, followed by drying at 100 °C for 24 hours to remove residual solvents. Finally, the dried gel was subjected to calcination at 1200 °C for 2 hours to enhance crystallinity and eliminate any remaining organic components, yielding the final Al_2O_3 NPs.

2.3 Preparation of Nanofluid

Nanofluids with 0.2%, 0.5%, and 1% volume concentrations of Al_2O_3 NPs were prepared using the sol-gel method. The synthesized NPs were then dispersed into a standard coolant, which was a 1:2 mixture of ethylene glycol and distilled water. To ensure uniform distribution of the NPs, each concentration of the nanofluid was stirred for four hours using a magnetic stirrer, facilitating proper dispersion and preventing particle agglomeration.

2.4 Characterization of NPs

Before applying NPs in practical scenarios, it is essential to assess their characteristics to determine if they are suitable for the intended application. To this end, the synthesized Al_2O_3 NPs were characterized using a UV-Vis spectrometer.

2.5 Mathematical Model

In analyzing the heat transfer behavior of the nanofluid, the collected data was mathematically modeled by treating the fluid as a Newtonian fluid. This classification is justified by the relatively low concentration of NPs dispersed in the base fluid, which results in an almost negligible impact on the fluid's viscosity. Since the viscosity remains largely unchanged, the fluid exhibits a consistent, linear relationship between shear stress and shear rate, characteristic of Newtonian behavior. Moreover, any significant increase in viscosity would be undesirable for practical automotive applications, as it would hinder the coolant's ability to flow efficiently through narrow tubes at high velocities. Elevated viscosity could increase flow resistance, reduce cooling efficiency, and place additional strain on the coolant pumping system. Therefore, maintaining a low NPs

concentration ensures both the physical feasibility and thermal performance of the nanofluid in real-world applications. The car used for testing was fitted with a tubular, cross-flow type radiator containing 47 vertical tubes made from aluminum.

- Specification of car radiator;
- Height of the radiator (h) = 0.450 m
- Length of radiator (l)=0.609m
- Thickness of fin (t)=0.025m
- Number of air passages = 99
- Tube thickness = 0.005mm
- Tube diameter = 10mm.

The radiator performance was analyzed using the Logarithmic Mean Temperature Difference (LMTD) as: method [27];

$$Q_{ave} = UAF \Delta T_{lm} \dots\dots\dots(1)$$

- Where,
- U = Overall heat transfer coefficient,
- A = Surface area, and
- F = Correction factor
- ΔT_{lm} = Log Mean Temperature Difference (LMTD)

which was given as;

$$\Delta T_{lm} = \frac{\Delta T_1 - \Delta T_2}{\ln(\Delta T_1 / \Delta T_2)} \dots\dots\dots(2)$$

where $\Delta T_1 = T_{c_i} - T_{a_i}$, $\Delta T_2 = T_{c_o} - T_{a_o}$

- Here,
- T_{c_i} = Inlet temperature of coolant
- T_{c_o} = Outlet temperature of coolant
- T_{a_i} = Inlet temperature of air
- T_{a_o} = Outlet temperature of air

Correction factor (F) is given by:

$$F = \frac{\ln(1 - RS) / (1 - S)}{(1 - 1/R)\ln[1 + R\ln(1 - S)]} \dots\dots\dots(3)$$

where R and S are dimensionless temperature ratios and are given as:

$$R = \frac{(T_{a_o} - T_{a_i})}{(T_{c_i} - T_{c_o})} \dots\dots\dots(4)$$

$$S = \frac{(T_{c_o} - T_{c_i})}{(T_{a_i} - T_{c_i})} \dots\dots\dots(5)$$

The average heat transfer rate was calculated as [28];

$$Q_{ave} = 0.5(Q_c + Q_a) \dots\dots\dots(6)$$

- Here,
- Q_{ave} = Average Heat transfer rate
- Q_c = Coolant Side Heat transfer rate
- Q_a = Heat Gained by air during the process
- Coolant side heat transfer rate (Q_c) was calculated

as:

$$Q_c = m_c C_{p_c} (T_{c_i} - T_{c_o}) \dots\dots\dots(7)$$

- Where,
- m_c = Mass flow rate of coolant,
- C_{p_c} = Specific heat of coolant.
- Similarly, heat gained by the air (Q_a) was calculates

$$Q_a = m_a C_{p_a} (T_{a_i} - T_{a_o}) \dots\dots\dots(8)$$

- Where,
- m_a = Mass flow rate of air,
- C_{p_a} = Specific heat of air.

In an ideal situation, heat lost by the coolant must be equal to the heat absorbed by the air. But this ideal condition is achieved due to several losses. This difference can be calculated by:

$$Heat\ balance_{ave} = \frac{Q_c - Q_a}{Q_{ave}} \times 100 \dots\dots(9)$$

Here, a and u correspondingly represent the total coolant and air inner surface area of the tubes and the overall heat transfer coefficient of the coolant and air sides.

Assumption

Table 1: Properties of NPs [29]

S. No.	Properties of NPs	Al_2O_3 NPs
--------	-------------------	---------------

1	Density (ρ_p)	3950 Kg/m ³
2	Specific heat (c_p)	873.336 J/kg.K
3	Thermal Conductivity (k_p)	31.922 W/m.K

3. Results and Discussion

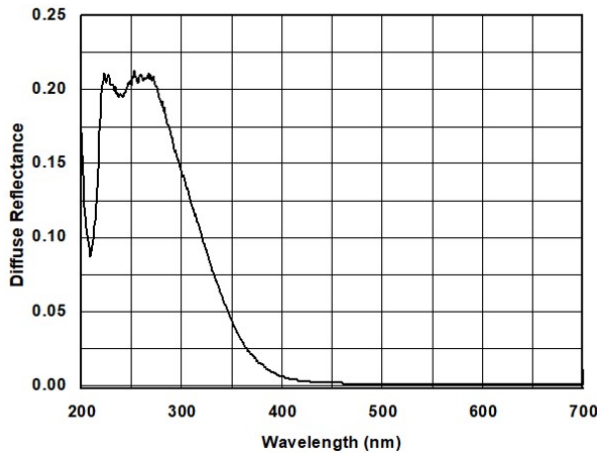


Figure 2: UV-Vis absorption of Al₂O₃ NPs

The UV-Vis absorption spectra of Al₂O₃ NPs are presented in Figure 2. The absorption peaks observed at 225 and 280 nm in the ultraviolet region confirm that the synthesized NPs are Al₂O₃ nanowires [30].

Following the UV-Vis absorption spectra analysis, the optical band gap was calculated using the Tauc formula. The band gap was determined by applying the absorption coefficient to the Tauc equation, and the band gap value was obtained from the Tauc plot as follows:

1. Equation of Tauc formula;

$$(h\nu\alpha)^{1/n} = A(h\nu - E_g) \dots \dots \dots (1)$$

Here,

h = Planck's constant,

α = Absorption coefficient,

A = Proportional constant

E_g = Optical band gap

ν = Frequency of vibration,

n = Tauc exponent

Tauc exponent value depends on the transition type, i.e.;

$n = 1/2$ for direct allowed transition

$n = 3/2$ for direct forbidden transition

$n = 2$ for indirect allowed transition

$n = 3$ for indirect forbidden transition

In this study, $n=1/2$, the direct permitted sample transition was used.

2. The energy band gap was measured using the Kubelka-Munk theory in conjunction with diffuse

reflectance spectra. In this approach, $F(R_\infty)$, was used to replace the absorption wavelength in the Tauc equation, enabling the calculation of the band gap. Thus, the equation becomes;

$$(h\nu F(R_\infty))^2 = A(h\nu - E_g) \dots \dots \dots (2)$$

Here, R_∞ is the sample reflection coefficient.

3. The graph was plotted between $(h\nu F(R_\infty))^2$ and $h\nu$ keeping $h\nu$ in horizontal and $(h\nu F(R_\infty))^2$ in vertical axis.

Here, $h\nu$ is expressed in terms of electron volts (eV) and wavelength (λ) nm is changed to $h\nu = 1239.7/\lambda$.

4. A tangent line from the point of inflection on the curve was drawn to find out the band gap of NPs.

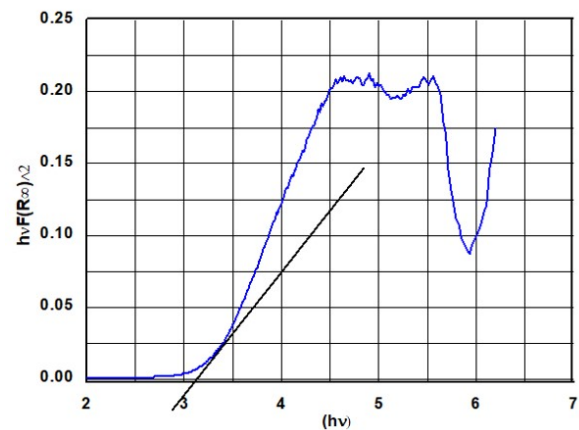


Figure 3: Band gap energy determination from the Tauc plot

In the Tauc plot Figure 3, the tangent line intersects the x-axis at a value of 3.23 eV, which corresponds to the band gap of the NPs. This, along with the absorption peaks at 225 nm and 289 nm, confirms the formation of Al₂O₃ NPs. The thermal performance of the vehicle radiator was then analyzed at a constant flow rate and the same Reynolds number for both the coolant and air sides. During the test, the engine speed was gradually increased up to 2500 rpm. To ensure the accuracy of the experimental setup, the reliability was first confirmed using the standard coolant.

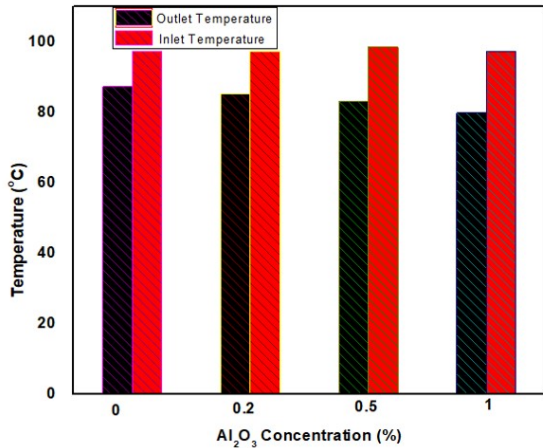


Figure 4: Inlet and outlet temperature of nanofluids at different concentrations of NPs

Figure 4 presents the inlet and outlet temperatures of nanofluids at various NPs concentrations. For the base fluid without NPs, the temperature decreased from 97.5 °C to 87.5 °C. With the addition of 0.2% NPs, the outlet temperature dropped further to 85.5 °C. At 0.5% concentration, it decreased to 83.31 °C. The most significant drop was observed at 1% NP concentration, where the temperature fell from 97.5 °C to 80 °C. This progressive decrease in outlet temperature suggests that the presence of NPs enhances molecular mobility within the fluid, thereby improving heat transfer efficiency and leading to more effective cooling [31].

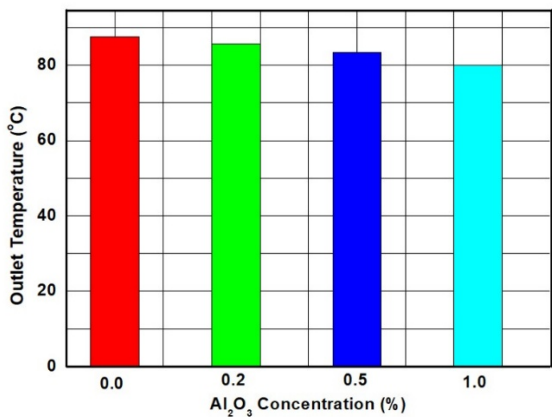


Figure 5: Effect of NPs concentration on outlet temperature

Figure 5 shows the outlet temperature of nanofluids at varying concentrations of NPs. The graphs indicate that the outlet temperature decreases with increasing NP concentration. The base coolant exhibited the highest outlet temperature, while the nanofluid with the highest NP concentration recorded the lowest. This trend suggests that the addition of NPs enhances the thermal properties of the coolant, allowing for more

efficient heat dissipation and resulting in lower outlet temperatures [32]. These results confirm that the presence of NPs improves the overall heat transfer performance of the fluid.

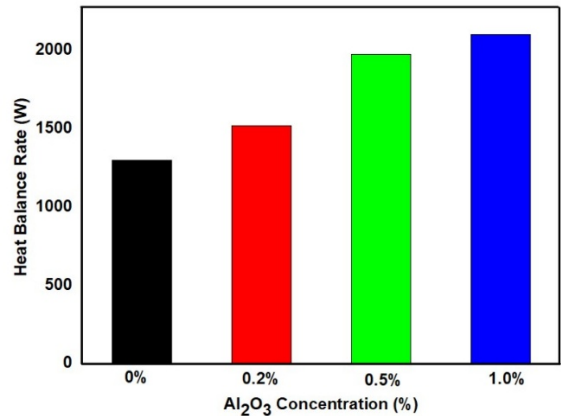


Figure 6: Effect of NPs concentration on heat transfer of coolant

Figure 6 illustrates the heat transfer rate at various concentrations of Al₂O₃ NPs. The base coolant exhibited the lowest heat transfer rate at 1280.60 W. With the addition of 0.2% NPs, the heat transfer rate increased by 28.92% to 1641.61 W. At 0.5% concentration, the enhancement was more significant, reaching a 52.16% increase (1948.59 W). Further increasing the concentration to 1% resulted in a 70.85% improvement, with a heat transfer rate of 2177.70 W. While the rate of improvement was notable up to 0.5%, the gains beyond that point were less substantial. Therefore, it can be concluded that increasing the NPs concentration up to 1% by volume is effective for enhancing thermal performance, with diminishing returns beyond 0.5%.

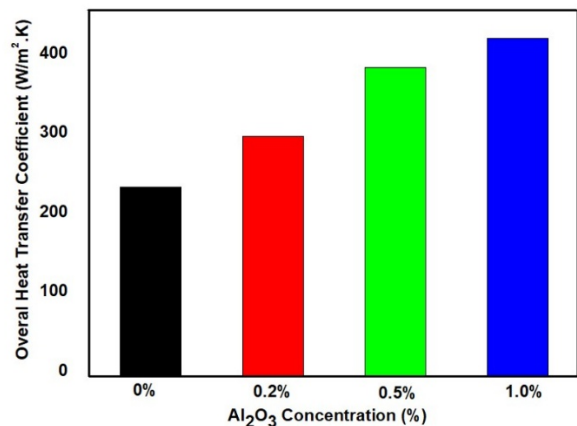


Figure 7: Effect of NPs concentration on overall heat transfer coefficient

Figure 7 depicts the trend of increasing overall heat transfer coefficient with rising concentrations of Al_2O_3 NPs in the coolant. The base fluid, without any NPs, exhibited an overall heat transfer coefficient of $236.036 \text{ W/m}^2\cdot\text{K}$. With the addition of 0.2% NPs by volume, this value increased by 33.63%, reaching $315.57 \text{ W/m}^2\cdot\text{K}$. At a 0.5% concentration, the enhancement rose to 65.4%, yielding a value of $390.42 \text{ W/m}^2\cdot\text{K}$. The maximum improvement was observed at 1% NP concentration, where the overall heat transfer coefficient increased by 83.5% to $433.32 \text{ W/m}^2\cdot\text{K}$.

This notable enhancement in thermal performance can be attributed to the intrinsic properties of NPs, particularly their high surface area-to-volume ratio, which facilitates more efficient thermal interaction with the surrounding fluid. Additionally, the Brownian motion of NPs promotes microscale fluid agitation, improving convective heat transfer and contributing to the observed increase in the overall heat transfer coefficient. These combined effects make NP-enhanced coolants a promising alternative for improving heat dissipation in thermal systems [33], [34].

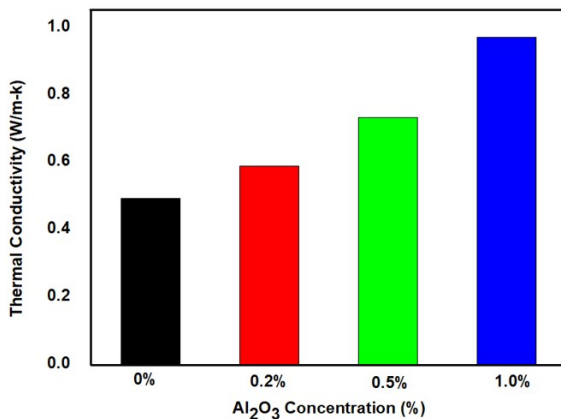


Figure 8: Effect of NPs concentration on thermal conductivity

Figure 8 illustrates the effect of NPs concentration on the thermal conductivity of the nanofluid, as calculated using the Maxwell-Eucken equation. The base fluid, without any NPs, exhibited an initial thermal conductivity of $0.4945 \text{ W/m}\cdot\text{K}$. Upon the addition of 0.2% Al_2O_3 NPs by volume, the thermal conductivity increased by 19.52%. This enhancement continued with higher concentrations—at 0.5%, thermal conductivity rose by 48.6%, reaching $0.7352 \text{ W/m}\cdot\text{K}$. The highest improvement was observed at 1% concentration, where thermal conductivity nearly doubled, increasing by 96.8% to $0.97356 \text{ W/m}\cdot\text{K}$.

This significant enhancement is primarily attributed to the unique thermal properties of NPs. NPs facilitate improved heat transfer by enabling phonon transport, where phonons (quantized thermal vibrations) scatter and experience extended mean-free paths. Additionally, the Brownian motion of NPs promotes microscale mixing within the fluid, further boosting thermal conductivity. In polymer-based fluids, the interaction between NPs and polymer chains leads to a more rigid molecular structure, which enhances the fluid's overall heat conduction capability. These mechanisms collectively contribute to the superior thermal performance of the nanofluid compared to the conventional coolant [35].

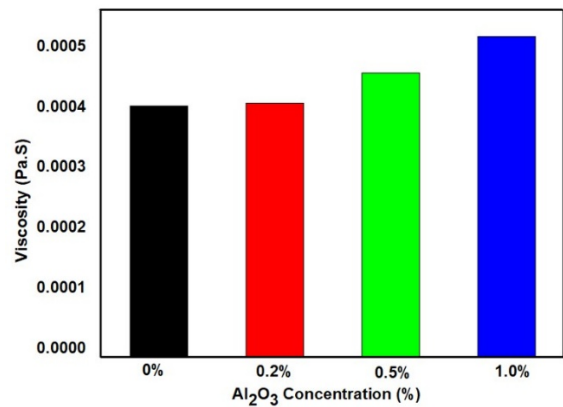


Figure 9: Effect of NPs concentration on Viscosity

Figure 9 illustrates the effect of NPs concentration on the viscosity of the fluid, as determined through analytical calculations. The base fluid exhibited the lowest viscosity, measured at $0.000415 \text{ Pa}\cdot\text{s}$, while the highest viscosity value of $0.000531 \text{ Pa}\cdot\text{s}$ was observed at a 1% volume concentration of Al_2O_3 NPs. The overall viscosity of the fluid remained relatively low across all concentrations, which further justifies the assumption of Newtonian behavior during the modeling of fluid flow.

The increase in viscosity at higher NP concentrations can be attributed to the formation of structured layers around the NPs within the liquid medium, which restricts the mobility of fluid molecules. This behavior indicates that the viscosity of nanofluids is influenced by multiple factors, including the shape, size, concentration, and surface properties of the NPs, as well as the intrinsic characteristics of the base fluid [36]. If the fluid were to be considered as non-Newtonian, its viscosity would need to be explicitly accounted for in the calculation of the heat transfer coefficient, as non-Newtonian fluids exhibit variable viscosity depending on

shear rate and flow conditions. However, in this particular case, the base viscosity of the nanofluid is inherently low. Additionally, the concentration of NPs introduced into the fluid is minimal, resulting in only a slight variation in viscosity. This marginal change is insufficient to cause any significant deviation in the thermal behavior of the fluid. As a result, the impact of viscosity on the overall heat transfer calculations remains negligible, and the assumption of Newtonian behavior does not compromise the accuracy or reliability of the obtained results.

Therefore, the results obtained remain accurate even when considering the Newtonian fluid model. The only potential sources of error that could influence the accuracy of the findings are primarily attributed to practical limitations in the experimental setup. These include head losses within the coolant tube due to friction and flow resistance, the presence of impurities or deposits inside the coolant passage that may alter flow characteristics and various dynamic factors associated with the experimental vehicle. Such dynamic factors encompass fluctuations in engine RPM, degradation of engine components over time, wear and tear in the coolant pumping system, and other real-world operating conditions that could slightly deviate the system's behavior from the idealized model.

4. Conclusion

In this experimental study, Al_2O_3 NPs were dispersed in a conventional engine coolant at volume concentrations of 0.2%, 0.5%, and 1% to investigate their impact on the heat transfer performance of nanofluids.

The following key conclusions were drawn from the research:

- Al_2O_3 NPs were successfully synthesized using the sol-gel method and subsequently characterized to confirm their structural and optical properties.
- The presence of a characteristic peak in the UV-Visible absorption spectra validated the formation of Al_2O_3 NPs.
- A noticeable reduction in outlet temperature was observed across all NPs concentrations, indicating improved heat absorption and dissipation characteristics of the nanofluids.
- At a NP concentration of 1% by volume, the heat transfer rate and the overall heat transfer coefficient increased significantly, by 70.85% and 83.5%, respectively, compared to the base coolant.

These findings demonstrate that incorporating Al_2O_3 NPs into the base fluid substantially enhances its thermal performance. Moreover, the degree of enhancement can be effectively tuned by adjusting the NPs concentration. This approach offers a promising advancement over conventional coolants, potentially leading to increased thermal efficiency, reduced engine overheating, and improved overall performance in automotive cooling systems.

Acknowledgements

We would like to express our gratitude to the Department of Mechanical and Aerospace Engineering, the Department of Applied Science and Chemical Engineering at Pulchowk Campus, and the TATA authorized center, SIPRADI Trading Pvt. Ltd., for providing the essential laboratories and facilities.

Declaration of interest

The authors declare that they have no known financial or personal conflicts of interest that could have influenced the work reported in this paper.

Competing interests

The authors declare no conflict of interest regarding the publication of this article.

References

- [1] RadoTD, "Heat transfer inside engine combustion chamber" Reference: <https://www.physicsforums.com/threads/heat-transfer-inside-engine-combustion-chamber.372374/>, *Phys. Forum*, 2010.
- [2] D. Sagar, G. Singh, and A. Agarwal, "Critique of Engine Material & Cooling System," pp. 2678–2684, 2015.
- [3] R. M. Stewart and T. W. Selby, "The relationship between oil viscosity and engine performance - a literature search.," *SAE Int.*, 1977.
- [4] M. Festus and D. E. Ben Hagan, "Analyzing the Effect of Cooling System on Temperature Using Modeling and Simulation with Reference to ICE Parameters," *Int. J. Emerg. Trends Eng. Dev.*, vol. 7, no. 6, 2017, doi: 10.26808/rs.ed.i7v6.11.
- [5] S. Sirsikar, V. Mehta, K. Chafekar, G. Sonawane, and Y. Dandekar, "Review Paper of Engine Cooling System," *Int. Res. J. Eng. Technol.*, pp. 4538–4541, 2020, [Online]. Available: www.irjet.net
- [6] W. N. Mutuku, "Ethylene glycol (EG)-based

- nanofluids as a coolant for automotive radiator," *Asia Pacific J. Comput. Eng.*, vol. 3, no. 1, 2016, doi: 10.1186/s40540-016-0017-3.
- [7] S. Eiamsa-ard, K. Kiatkittipong, and W. Jedsadaratanachai, "Heat transfer enhancement of TiO₂/water nanofluid in a heat exchanger tube equipped with overlapped dual twisted-tapes," *Eng. Sci. Technol. an Int. J.*, vol. 18, no. 3, pp. 336–350, 2015, doi: 10.1016/j.jestch.2015.01.008.
- [8] R. S. Vajjha, D. K. Das, and P. K. Namburu, "Numerical study of fluid dynamic and heat transfer performance of Al₂O₃ and CuO nanofluids in the flat tubes of a radiator," *Int. J. Heat Fluid Flow*, vol. 31, no. 4, pp. 613–621, 2010, doi: 10.1016/j.ijheatfluidflow.2010.02.016.
- [9] A. Kumar, M. A. Hassan, and P. Chand, "Heat transport in nanofluid coolant car radiator with louvered fins," *Powder Technol.*, vol. 376, pp. 631–642, 2020, doi: 10.1016/j.powtec.2020.08.047.
- [10] T. T. Loong, H. Salleh, A. Khalid, and H. Koten, "Thermal performance evaluation for different type of metal oxide water based nanofluids," *Case Stud. Therm. Eng.*, vol. 27, 2021, doi: 10.1016/j.csite.2021.101288.
- [11] G. J. Owens, R. K. Singh, F. Foroutan, M. Alqaysi, C. M. Han, C. M., H. W. Kim, J. C. Knowles, "Sol-gel based materials for biomedical applications," *Prog. Mater. Sci.*, vol. 77, pp. 1–79, 2016, doi: 10.1016/j.pmatsci.2015.12.001.
- [12] I. A. Rahman and V. Padavettan, "Synthesis of Silica nanoparticles by Sol-Gel: Size-dependent properties, surface modification, and applications in silica-polymer nanocomposites a review," *J. Nanomater.*, vol. 2012, 2012, doi: 10.1155/2012/132424.
- [13] M. Catauro, E. Tranquillo, G. Dal Poggetto, M. Pasquali, A. Dell'Era, and S. V. Cipriotti, "Influence of the heat treatment on the particles size and on the crystalline phase of TiO₂ synthesized by the sol-gel method," *Materials (Basel)*, vol. 11, no. 12, 2018, doi: 10.3390/ma11122364.
- [14] S. L. Isley and R. L. Penn, "Titanium dioxide nanoparticles: Effect of sol-gel pH on phase composition, particle size, and particle growth mechanism," *J. Phys. Chem. C*, vol. 112, no. 12, pp. 4469–4474, 2008, doi: 10.1021/jp710844d.
- [15] L. L. Hench, "The sol-gel process," *Chem. Rev.*, 1990.
- [16] K. C. Ghosh, C.S. Popuri, U. Thupakula, "Preparation of nanocrystalline CuAlO₂ through sol-gel route," *J. Sol-gel Sci. Technol. - J SOL-GEL SCI TECHNOL*, vol. 52, no. 75–81, 2009.
- [17] S. Tabesh, F. Davar, and M. R. Loghman-Estarki, "Preparation of γ -Al₂O₃ nanoparticles using modified sol-gel method and its use for the adsorption of lead and cadmium ions," *J. Alloys Compd.*, vol. 730, pp. 441–449, 2018, doi: 10.1016/j.jallcom.2017.09.246.
- [18] D. Chavan and A. T. Pise, "Performance investigation of an automotive car radiator operated with nanofluid as a coolant," *J. Therm. Sci. Eng. Appl.*, vol. 6, no. 2, 2013, doi: 10.1115/1.4025230.
- [19] M. M. Elias, I. M. Mahbubul, R. Saidur, M. R. Sohel, I. M. Shahrul, S. S. Khalrduzzaman, S. Sadeghipour, "Experimental investigation on the thermo-physical properties of Al₂O₃ nanoparticles suspended in car radiator coolant," *Int. Commun. Heat Mass Transf.*, vol. 54, pp. 48–53, 2014, doi: 10.1016/j.icheatmasstransfer.2014.03.005.
- [20] K. P. Vasudevan Nambeesan, R. Parthiban, K. Ram Kumar, U. R. Athul, M. Vivek, and S. Thirumalini, "Experimental study of heat transfer enhancement in automobile radiator using Al₂O₃/water-ethylene glycol nanofluid coolants," *Int. J. Automot. Mech. Eng.*, vol. 12, no. 1, pp. 2857–2865, 2015, doi: 10.15282/ijame.12.2015.5.0240.
- [21] H. Xie, J. Wang, T. Xi, Y. Liu, F. Ai, and Q. Wu, "Thermal conductivity enhancement of suspensions containing nanosized alumina particles," *J. Appl. Phys.*, vol. 91, no. 7, pp. 4568–4572, 2002, doi: 10.1063/1.1454184.
- [22] S. Mukherjee, T. Halder, S. Ranjan, K. Bose, P. C. Mishra, and S. Chakrabarty, "Effects of SiO₂ nanoparticles addition on performance of commercial engine coolant: Experimental investigation and empirical correlation," *Energy*, vol. 231, 2021, doi: 10.1016/j.energy.2021.120913.
- [23] J. A. Eastman, S. U. S. Choi, S. Li, W. Yu, and L. J. Thompson, "Anomalously increased effective thermal conductivities of ethylene glycol-based nanofluids containing copper nanoparticles," *Appl. Phys. Lett.*, vol. 78, no. 6, pp. 718–720, 2001, doi: 10.1063/1.1341218.
- [24] S. M. Peyghambarzadeh, S. H. Hashemabadi, S. M. Hoseini, and M. Seifi Jamnani, "Experimental study of heat transfer enhancement using water/ethylene glycol based nanofluids as a new coolant for car radiators," *Int. Commun. Heat Mass Transf.*, vol. 38, no. 9, pp. 1283–1290, 2011, doi: 10.1016/j.icheatmasstransfer.2011.07.001.
- [25] H. M. Ali, M. D. Azhar, M. Saleem, Q. S. Saeed, and A.

- Saieed, "Heat transfer enhancement of car radiator using aqua based magnesium oxide nanofluids," *Therm. Sci.*, vol. 19, no. 6, pp. 2039–2048, 2015, doi: 10.2298/TSCI150526130A.
- [26] D. Wen and Y. Ding, "Experimental investigation into convective heat transfer of nanofluids at the entrance region under laminar flow conditions," *Int. J. Heat Mass Transf.*, vol. 47, no. 24, pp. 5181–5188, 2004, doi: 10.1016/j.ijheatmasstransfer.2004.07.012.
- [27] M. Ali, A. M. El-Leathy, and Z. Al-Sofyany, "The effect of nanofluid concentration on the cooling system of vehicles radiator," *Adv. Mech. Eng.*, vol. 2014, 2014, doi: 10.1155/2014/962510.
- [28] S. Vithayasai, T. Kiatsiriroat, and A. Nuntaphan, "Effect of electric field on heat transfer performance of automobile radiator at low frontal air velocity," *Appl. Therm. Eng.*, vol. 26, no. 17–18, pp. 2073–2078, 2006, doi: 10.1016/j.applthermaleng.2006.04.018.
- [29] R. A. Bhogare and B. S. Kothawale, "Performance investigation of Automobile Radiator operated with Al₂O₃ based nanofluid," *IOSR J. Mech. Civ. Eng.*, vol. 11, no. 3, pp. 23–30, 2014, doi: 10.9790/1684-11352330.
- [30] X. S. Peng, L. D. Zhang, G. W. Meng, X. F. Wang, C. Z. Wang, G. S. Wu, "Photoluminescence and infrared properties of α -Al₂O₃ nanowires and nanobelts," *J. Phys. Chem. B*, vol. 106, no. 43, pp. 11163–11167, 2002, doi: 10.1021/jp026028+.
- [31] A. S. M. Aljaloud, K. Smida, H. F. M. Ameen, M. A. Albedah, and I. Tlili, "Investigation of phase change and heat transfer in water/copper oxide nanofluid enclosed in a cylindrical tank with porous medium: A molecular dynamics approach," *Eng. Anal. Bound. Elem.*, vol. 146, pp. 284–291, 2023, doi: 10.1016/j.enganabound.2022.10.034.
- [32] L. Zhang, L. Tian, Y. Jing, P. Qu, and A. Zhang, "Molecular dynamics study on the mechanism of nanofluid coolant's thermal conductivity improvement," *J. Mol. Liq.*, vol. 345, 2022, doi: 10.1016/j.molliq.2021.118228.
- [33] G. Nobrega, R. R. de Souza, I. M. Gonçalves, A. S. Moita, J. E. Ribeiro, and R. A. Lima, "Recent Developments on the Thermal Properties, Stability and Applications of Nanofluids in Machining, Solar Energy and Biomedicine," *Appl. Sci.*, vol. 12, no. 3, 2022, doi: 10.3390/app12031115.
- [34] S. A. Angayarkanni and J. Philip, "Review on thermal properties of nanofluids: Recent developments," *Adv. Colloid Interface Sci.*, vol. 225, pp. 146–176, 2015, doi: 10.1016/j.cis.2015.08.014.
- [35] D. Song, D. Jing, W. Ma, and X. Zhang, "Effect of particle aggregation on thermal conductivity of nanofluids: Enhancement of phonon MFP," *J. Appl. Phys.*, vol. 125, no. 1, 2019, doi: 10.1063/1.5062600.
- [36] L. Shan, D. J. Jasim, S. M. Sajadi, A. D. J. Al-Bayati, N. Ahmad, N. N. Esfahani, B. M. Ridha, A. H. Alsalamy, H. H. Afrouzi, Sh. Baghaei, "Comprehensive analysis of dispersion and aggregation morphology of nanoparticles on the thermophysical properties of water-based nanofluids using molecular dynamics simulation," *J. Taiwan Inst. Chem. Eng.*, vol. 150, 2023, doi: 10.1016/j.jtice.2023.105043.